Regulation of Root Nitrate Uptake at the NRT2.1 Protein Level in Arabidopsis thaliana.

Judith Wirth, Franck Chopin, Véronique Santoni, Gaëlle Viennois, Pascal Tillard, Anne Krapp, Laurence Lejay, Francoise Daniel-Vedele, Alain Gojon

THE JOURNAL OF BIOLOGICAL CHEMISTRY VOL. 282, NO. 32, pp. 23541–23552, August 10, 2007

Regulation of Root Nitrate Uptake at the NRT2.1 Protein Level in *Arabidopsis thaliana*[*][S]

Received for publication, January 31, 2007, and in revised form, June 14, 2007 Published, JBC Papers in Press, June 15, 2007, DOI 10.1074/jbc.M700901200

Judith Wirth[‡1], Franck Chopin[§1], Véronique Santoni[‡], Gaëlle Viennois[‡], Pascal Tillard[‡], Anne Krapp[§], Laurence Lejay[‡2], Françoise Daniel-Vedele[§], and Alain Gojon[‡]

From the [‡]Institut de Biologie Intégrative des Plantes, UMR 5004, Biochimie et Physiologie Moléculaire des Plantes, CNRS/INRA/SupAgro/UM2, Place Viala, F-34060 Montpellier, France and the [§]Unité de Nutrition Azotée des Plantes, INRA, route de St. Cyr, F-78026 Versailles, France

In *Arabidopsis* the *NRT2.1* gene encodes a main component of the root high-affinity nitrate uptake system (HATS). Its regulation has been thoroughly studied showing a strong correlation between *NRT2.1* expression and HATS activity. Despite its central role in plant nutrition, nothing is known concerning localization and regulation of NRT2.1 at the protein level. By combining a green fluorescent protein fusion strategy and an immunological approach, we show that NRT2.1 is mainly localized in the plasma membrane of root cortical and epidermal cells, and that several forms of the protein seems to co-exist in cell membranes (the monomer and at least one higher molecular weight complex). The monomer is the most abundant form of NRT2.1, and seems to be the one involved in NO_3^- transport. It strictly requires the NAR2.1 protein to be expressed and addressed at the plasma membrane. No rapid changes in NRT2.1 abundance were observed in response to light, sucrose, or nitrogen treatments that strongly affect both *NRT2.1* mRNA level and HATS activity. This suggests the occurrence of post-translational regulatory mechanisms. One such mechanism could correspond to the cleavage of NRT2.1 C terminus, which results in the presence of both intact and truncated proteins in the plasma membrane.

The *NRT2.1* gene of *Arabidopsis thaliana* is part of a small multigene family comprising 7 members, which with the exception of *NRT2.7*, are predominantly expressed in the roots (1, 2). *NRT2* genes are found in a large variety of organisms (fungi, certain yeasts, green algae, and plants) and belong to the nitrate nitrite porter family of transporter genes (3).

It is generally assumed that *NRT2* genes encode high-affinity nitrate (NO_3^-) or nitrite transporters (4–11), and that in higher plants, they play a key role in the root high-affinity transport system (HATS),[3] which ensures uptake of NO_3^- from the soil solution (3, 12–14). In all plant species investigated to date, the NO_3^- HATS displays a saturable activity, with a V_{max} generally reached for NO_3^- concentrations comprised between 0.2 and 0.5 mM (3, 12, 14). Although the functional characterization of almost all higher plant NRT2 transporters remains to be done, it is now well documented that NRT2.1 is a major component of the HATS in *A. thaliana* as shown by the fact that (i) of the seven *NRT2* members, only *NRT2.1* transcript abundance showed significant correlation ($r^2 = 0.74$) with HATS activity (2, 11) and (ii) several mutants disrupted for the *NRT2.1* gene (15, 16) or for both *NRT2.1–NRT2.2* genes (17, 18) have lost up to 75% of the high-affinity NO_3^- uptake activity. As a consequence, growth of these mutants is severely impaired at low NO_3^- concentration (15, 19, 20), but not at high NO_3^- concentration when low-affinity transporters, most probably those of the NRT1 family (3, 12, 14), are active.

Despite its firmly established role in root NO_3^- uptake, several aspects of NRT2.1 function remain enigmatic. First, unlike the *Aspergillus nidulans* or *Chlorella sorokiniana* NRT2 transporters (CRNA or ChNRT2.1, respectively) (21, 22), but similarly to NRT2 proteins of *Chlamydomonas reinhardtii*, NRT2.1 does not seem to be able to mediate NO_3^- transport on its own. In *Xenopus* oocytes, CrNRT2 and AtNRT2.1 (as well as its *Hordeum vulgare* homologue, HvNRT2.1) need to be co-expressed with a NAR2 protein, to yield NO_3^- transport (19, 23, 24). This has suggested that the actual transport system corresponds in fact to a dual component (NRT2/NAR2) transporter (19, 24). Indeed, a crucial role of the NRT2.1 putative partner, NAR2.1 (also called NRT3.1), is confirmed by the observation that mutants disrupted in the *NAR2.1* gene (At5g50200) display an even stronger defect in HATS activity than the *NRT2.1* mutants in *Arabidopsis* (19, 25). A second surprising aspect of NRT2.1 function is that it seems to be involved in the control of lateral root initiation, in a way that is independent from its transport activity (16, 26). Because NO_3^- is not only a major nitrogen source for nutrition of the plants, but also acts as a signal to modulate plant metabolism and development (27, 28), this gave rise to the hypothesis that NRT2.1 may also be a NO_3^- sensor, or a signal transducer (16).

The regulation of NRT2.1 expression has been thoroughly investigated at the mRNA level. *NRT2.1* transcript accumulation predominantly occurs in epidermis and cortex of the

[*] This work was supported by European Union program PLUSN Grant HPRN-CT-2002-00247. The costs of publication of this article were defrayed in part by the payment of page charges. This article must therefore be hereby marked "*advertisement*" in accordance with 18 U.S.C. Section 1734 solely to indicate this fact.

[S] The on-line version of this article (available at http://www.jbc.org) contains supplemental Figs. S1–S4.

[1] Both authors contributed equally to this work.

[2] To whom correspondence should be addressed. Tel.: 33-499-612-602; Fax: 33-467-525-737; E-mail: lejay@supagro.inra.fr.

[3] The abbreviations used are: HATS, high-affinity transport system; GFP, green fluorescent protein; MES, 4-morpholineethanesulfonic acid; ER, endoplasmic reticulum; ELISA, enzyme-linked immunosorbent assay; PM, plasma membrane; WT, wild type; PIP2, plasma membrane intrinsic protein.

mature root regions (29), and is affected by a wide range of environmental changes. Expression of *NRT2.1* is induced by low NO_3^- concentration (2, 4, 11, 30), feedback repressed by NH_4^+ and amino acids (11, 29–31), and stimulated by light and sugars (30, 32). These mechanisms are postulated to modulate root NO_3^- uptake as a function of both nitrogen and carbon status of the plant. More recently, *NRT2.1* has been shown to be down-regulated by NO_3^- itself, through a mechanism independent of the feedback repression exerted by nitrogen metabolites, but specifically triggered by the dual-affinity NRT1.1 NO_3^- transporter (33, 34). The NO_3^- HATS is subjected to the same controls, and in all cases, a strong correlation was found between the changes in *NRT2.1* transcript level and those in NO_3^- HATS activity, suggesting that the transcriptional regulation of *NRT2.1* expression plays a major role in governing root high-affinity NO_3^- uptake.

However, a yet limited number of reports suggest that post-transcriptional regulation of NRT2 transporters may also participate to the modulation of root NO_3^- uptake in response to environmental changes. In *Nicotiana plumbaginifolia* ectopic overexpression of the *NpNRT2.1* gene did not prevent the inhibition of root NO_3^- uptake by exogenous NH_4^+ supply (35). Likewise, in barley NH_4^+ accumulation in roots of plants treated with the glutamine synthetase inhibitor methionine sulfoximine decreased root NO_3^- uptake but did not change *HvNRT2.1* transcript level (36). Further evidence for post-translational control of NRT2 transporters is provided by the recent report on YNT1 in the yeast *Hansenula polymorpha*, showing that this protein undergoes trafficking to the vacuole and proteolysis in response to glutamine supply (37).

To gain further insights on NRT2.1 at the protein level in *Arabidopsis* we initiated the biochemical characterization of its localization and regulation, by combining a GFP fusion strategy and an immunological investigation. Our results provide strong evidence that NRT2.1 is predominantly localized in the plasma membrane of root cortical and epidermal cells of the mature regions of the roots, and show that NAR2.1 is essential for NRT2.1 expression. They also reveal that several forms of the protein seem to co-exist in the plasma membrane. Furthermore, treatments, which rapidly modulate both *NRT2.1* transcript level and NO_3^- HATS activity, are shown to yield only very slow responses of the NRT2.1 protein, suggesting the occurrence of important post-translational regulatory mechanisms. One such putative mechanism is unraveled, which could be associated with partial proteolysis of NRT2.1 resulting in the cleavage of the C terminus of the protein.

EXPERIMENTAL PROCEDURES

Production of the $P_{NRT2.1}$-NRT2.1-GFP Construct—Cloning of $P_{NRT2.1}$-*NRT2.1* (3114 bp, including the 1335-bp 5′ untranslated region and promoting sequence upstream the ATG) and fusion with *GFP* coding sequence at the 3′ end of *NRT2.1* was performed using Gateway™ Technology, according to the manufacturer's instructions (Gateway cloning manual, Invitrogen). The primers NRT2.1 GATE forward (CACCCACGTCAGCGAGATTGATCG) and NRT2.1 GATE reverse (AACATTGTTGGGTGTGTTCTCAGGC) were used to amplify the $P_{NRT2.1}$-*NRT2.1* complete DNA sequence from the *bac* clone T6D22 (ARBC, Columbus, OH). After gel purification of the PCR product with the Nucleo Spin® Extract Kit (Machery Nagel), $P_{NRT2.1}$-*NRT2.1* was cloned into the pENTR™/D-Topo vector (Invitrogen) to create an entry clone. After transformation of One Shot TOP10 thermocompetent *Escherichia coli* (Invitrogen) the vector was sequenced. LR (Invitrogen) reaction was performed to transfer $P_{NRT2.1}$-*NRT2.1* from entry clone to the destination binary vector pGWB4 (no promoter, C-sGFP) obtained from Tsuyoshi Nakagawa (Research Institute of Molecular Genetics, Shimane University, Matsue, Japan). Following the LR reaction thermocompetent DH5α *E. coli* were transformed and positive clones were selected with hygromycin. Prior transformation of *Agrobacterium*, part of the expression construct was sequenced to verify the translational fusion of $P_{NRT2.1}$-*NRT2.1* with the GFP tag. In addition we used plants, called P43NRT2.1, transformed with NRT2.1 fused to GFP in N-terminal, under the control of the ^{35}S promoter as described in Chopin *et al.* (38).

Plant Transformation—Binary vectors containing the GFP fusion construct were introduced into *Agrobacterium tumefaciens* strain GC3101. *A. thaliana nrt2.1-1* mutant plants, ecotype Wassilewskija (18), were transformed by dipping the flowers in the presence of Silwet L77 (39). The transformants were selected on a medium containing 30 mg/liter of hygromycin. For further analyses, T1 segregation ratios were analyzed to select transformants with one T-DNA insertion and to isolate T3-homozygous plants.

Growth Conditions—For all experiments, except those devoted to confocal imaging, plants were grown hydroponically using the experimental set-up described previously (30). Briefly, seeds were sown directly on the surface of wet sand in modified 1.5-ml microcentrifuge tubes, with the bottom replaced by a metal screen. The tubes supporting the seeds were placed on polystyrene floating rafts, on the surface of a 10-liter tank filled with tap water. The culture was then performed in a controlled growth chamber with 8 h/16 h day/night cycle at 24/20 °C. Light intensity during the light period was at 250 μmol m^{-2} s^{-1}. One week after sowing, the tap water was replaced by nutrient solution until the age of 6–7 weeks depending on the size of the plants. The basal nutrient solutions supplied to the plants are those described by Gansel *et al.* (31) and contained either 0.3 mM NO_3^-, 1 mM NO_3^-, 5 mM NO_3^-, or 10 mM NH_4NO_3 as nitrogen source. The nutrient solution was replaced every week during this period and the day before the experiment.

For confocal imaging, plants were grown in sterile conditions in vertical agar plates (12 × 12 cm) on the same basal medium as used for hydroponic cultures plus 2.5 mM MES and 1.2% (w/v) agar type A (Sigma, product A4550). It contained 1 mM NO_3^- as nitrogen source and either 3% sucrose (w/v) or no sugar. The pH was adjusted to 5.8 with KOH. After sowing, the plates were transferred in a growth chamber with 16 h/8 h day/night cycle at 21/18 °C and 70% relative humidity. Light intensity during the light period was at 125 μmol m^{-2} s^{-1}. Observations were performed after 14 days of growth.

In Vivo Protein Cross-linking—According to Rohila *et al.* (40) *in vivo* protein cross-linking was performed by adding formaldehyde to the nutrient solution of hydroponically grown plants

to get a final concentration of 1% (v/v). Plants were treated during 45 min before harvesting the roots for plasma membrane (PM) extraction.

Confocal Microscopy—GFP images were acquired with a Zeiss LSM 510 axiovert 200M inverted microscope. GFP (excitation/emission maxima ~488/507 nm) was excited with the 488 nm line of an Argon laser and detected via a 505–530 nm bandpass filter (green). Autofluorescence was detected via a 650-nm long pass filter (red). Dichroic mirrors used were HFT 488 and NFT 545.

To visualize the different plant cell membranes, several stains were used. Images of the plasma membrane and the tonoplast were obtained after 5 min and at least 16 h of incubation with 8.2 μM of the endocytic tracer FM4-64 (Invitrogen, product F34653), respectively. The endoplasmic reticulum was visualized after 30 min staining with 5 μM endoplasmic reticulum (ER) Tracker (Blue-White DPX, Invitrogen). FM4-64 was visualized with the microscope used for GFP imaging. FM4-64 (excitation/emission maxima ~515/640 nm) was excited with the 543-nm line and detected via LP 650 and LP 585, respectively. Dichroic mirrors used were HFT 488/543 and NFT 545. ER Tracker (excitation/emission maxima ~347–640 nm) images were obtained with the Zeiss LSM 510 Meta Axioplan 2 microscope. ER Tracker was excited with the diode 405-nm laser for blue dye and detected via a 420–480 BP filter (blue). Dichroic mirrors used were HFT 405/488/543 and NFT 490.

NRT2.1 Immunodetection and Membrane Purification—Root total proteins were extracted as described by Santoni *et al.* (41). Microsomes were prepared as described by Giannini *et al.* (42) and plasma membrane vesicles were purified from microsomes by aqueous two-phase partitioning, as described by Santoni *et al.* (43).

Proteins were separated on denaturing SDS-PAGE followed by an electrotransfer at 4 °C onto a nitrocellulose membrane (0.2 μM, Sartorius, Göttingen, Germany). NRT2.1 was detected using two different anti-NRT2.1 antisera produced by Eurogentec (Liège, Belgium) against either the synthetic peptide TLEKAGEVAKDKFGK (anti-NRT2.1 19) or CKNMHQGSLRFAENAK (anti-NRT2.1 20) (Fig. 2*A*). The two polyclonal antisera were affinity purified by Eurogentec. The immunodetection was performed with a chemiluminescent detection system kit (SuperSignal, Pierce).

For ELISA, serial 2-fold dilutions in a carbonate buffer (30 mM Na_2CO_3, 60 mM $NaHCO_3$, pH 9.5) of 500 ng of PM proteins were loaded in duplicate on Maxisorb immunoplates (Nunc, Denmark) and left overnight at 4 °C. The immunodetection was performed according to the manufacturer's instructions. The primary anti-NRT2.1 20 antibody (1:2500 dilution) and a secondary peroxidase-coupled anti-rabbit antibody were successively applied for 2 h at 37 °C. A linear regression between the absorbance signal due to oxidized 2,2′-azinobis-3-ethylbenzothiazoline-6-sulfonic acid diammonium salt, as read with a multiplate reader (Victor, PerkinElmer Life Sciences), and the amount of proteins was obtained for each sample and used for relative comparison between samples.

RNA Extraction and Reverse Transcription—RNA extraction was performed on roots as described previously (44) using guanidine hydrochloride and lithium chloride. Subsequently 40 μg of RNA were treated with DNase (RNase Free DNase Kit, Qiagen) and purified (RNeasy MinElute^{TM} Cleanup Kit, Qiagen) following the manufacturer's instructions. The absence of genomic DNA was verified by PCR using specific primers spanning an intron in the gene *APTR* (At1g27450).

Reverse transcription was performed with 4 μg of purified RNA and oligo$(dT)_{18}$ primers. The mixture was heated for 5 min at 72 °C and progressively (−1 °C per 10 s) cooled down to allow hybridization of the primers. The reaction was carried out in a volume of 20 μl in the presence of 200 units of Moloney murine leukemia virus reverse transcriptase (Promega) at 42 °C during 90 min. The quality of the cDNA was verified by PCR using the primers for the gene *APTR*.

Quantitative PCR—Real-time amplification was performed in a LightCycler (Roche Diagnostics) with the kit SYBR Green (LightCycler FastStart DNA Master SYBR Green1, Roche Diagnostics) according to the manufacturer's instructions with 1 μl of cDNA in a total volume of 10 μl. The following conditions of amplifications were applied: 10 min at 95 °C; 45 cycles of 5 s at 95 °C; 7 s at 65 °C; and 8 s at 72 °C. A melting curve was then performed to verify the specificity of the amplification. Successive dilutions of one sample were used as a standard curve. Amplification efficiency was around 1. All the results presented were standardized using the housekeeping gene Clathrin (At4g24550). The primers used were: NRT2.1 forward, AACAAGGGCTAACGTGGATG; NRT2.1 reverse, CTGCTTCTCCTGCTCATTCC; Clath forward, AGCATACACTGCGTGCAAAG; Clath reverse, TCGCCTGTGTCACATATCTC.

Root NO_3^- Influx Measurements—Root $^{15}NO_3^-$ influx was assayed as described by Dehlon *et al.* (45). Briefly, the plants were sequentially transferred to 0.1 mM $CaSO_4$ for 1 min, to complete nutrient solution, pH 5.8, containing 0.2 mM $^{15}NO_3^-$ (99 atom % excess ^{15}N) for 5 min, and finally to 0.1 mM $CaSO_4$ for 1 min. Roots were then separated from shoots, and the organs dried at 70 °C for 48 h. After determination of their dry weight, the samples were analyzed for total nitrogen and atom % ^{15}N using a continuous flow isotope ratio mass spectrometer coupled with a C/N elemental analyzer (model ANCA-MS; PDZ Europa, Crewe, UK) as described in Clarkson *et al.* (46). Each influx value is the mean of 6 to 12 replicates.

RESULTS

Tissular and Subcellular Localization of NRT2.1—To investigate the localization of NRT2.1 in the roots, NRT2.1-GFP transgenic lines were generated by expressing a GFP-tagged NRT2.1 protein (C-terminal translational fusion) in the *nrt2.1-1* knock-out mutant of *NRT2.1*. The GFP coding sequence was fused in-frame to the 3′ end of the *NRT2.1* gene under the control of its own promoter. Two transgenic lines (GFP10 and GFP12) displayed both a correct regulation of the expression of the transgene and a functional complementation of the mutant phenotype (supplemental materials Fig. S1). In these lines, the expression of $P_{NRT2.1}$-*NRT2.1-GFP* was induced by both light and sucrose in the roots, as it was the case for *NRT2.1* in WT plants. The NO_3^- HATS activity, determined by root $^{15}NO_3^-$ influx assays (0.2 mM external $^{15}NO_3^-$ concentration), was also stimulated by the light/sucrose treatments in

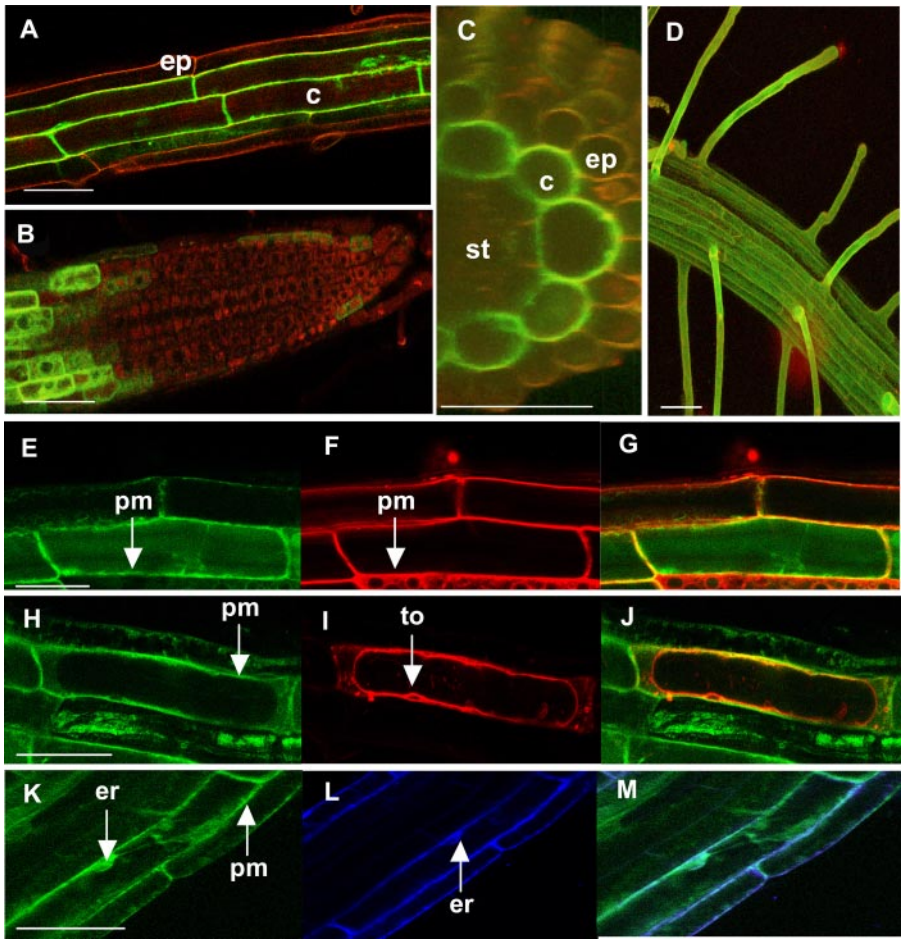

FIGURE 1. **Cellular and subcellular localization of NRT2.1-GFP in the transgenic line GFP10 expressing the $P_{NRT2.1}$-*NRT2.1-GFP* fusion gene.** Plants were grown in vertical Petri dishes for 14 days. *A*, longitudinal view; *C*, cross-section of a mature root. The abbreviations are: *ep*, epidermis; *c*, cortex; *st*, stele. *B*, longitudinal view of the apex. *D*, longitudinal view in three dimensions of a root of 6-week-old hydroponically grown plants. Root cells were stained for 5 min (*F*) or 16 h (*I*) with FM4-64 and for 30 min (*L*) with ER Tracker. The abbreviations used are: *pm*, plasma membrane; *to*, tonoplast; *er*, endoplasmatic reticulum. *E*, *H*, and *K* show the corresponding GFP signals, and *G*, *J*, and *M* represent overlays of the GFP and marker images. *Bar* = 50 μm.

both GFP10 and GFP12 plants, and restored at higher values than those measured in the *nrt2.1-1* mutant.

Cell-type specific expression of NRT2.1-GFP was therefore studied by confocal microscopy in both GFP10 and GFP12 plants grown *in vitro*. In roots of GFP10 plants, GFP fluorescence was mainly localized in the cortical cells along the primary and secondary roots (Fig. 1, *A* and *C*), except in the apical part of these roots where GFP was not present (Fig. 1*B*). No fluorescence was detected in the stele of the roots (Fig. 1*C*), and in the leaves (results not shown). These results were confirmed using the GFP12 line (data not shown). In plants grown hydroponically, NRT2.1-GFP was also found in mature regions of the roots, where in addition to the cortex, it was also expressed in the epidermal cells, and in root hairs (Fig. 1*D*).

The subcellular localization of the NRT2.1-GFP protein was investigated in roots of plants grown *in vitro*, using specific markers for cellular membranes. The PM and the tonoplast were visualized after a short and a long incubation with the red fluorescent dye FM4-64, respectively (47). After a short incubation time (5 min), FM4-64 fluorescence co-localized with that recorded from NRT2.1-GFP, yielding a yellow staining of the PM in the overlaid image (Fig. 1, *E–G*). After a prolonged incubation time (16 h), FM4-64 fluorescence had entirely moved to the tonoplast and became clearly distinguishable from the GFP fluorescence in the overlaid image (Fig. 1, *H–J*). Finally, to test the presence of NRT2.1-GFP in the ER, plants were treated with the vital ER Tracker blue-white DPX. Images showed blue staining of the ER around the nucleus, which co-localized with NRT2.1-GFP fluorescence in the overlaid image (Fig. 1, *K–M*). Despite the fact that the spatial resolution of these images may not be sufficient to allocate NRT2.1 to one specific membrane, they do show that NRT2.1 is not in the tonoplast, and suggest that this protein is localized in both the PM and ER.

Immunochemical Characterization of NRT2.1 in Root Cell Membranes—To further investigate NRT2.1 at the protein level, two specific polyclonal antibodies, called anti-NRT2.1 19 and anti-NRT2.1 20, were raised in rabbit against specific peptidic sequences within, respectively, an internal loop and the C terminus of the protein (Fig. 2*A*). The affinity-purified anti-NRT2.1 antibodies were tested on Western blots with total microsomal membranes purified from roots of hydroponically grown WT plants or *nrt2.1-1* and *nrt2.1-2* knock-out mutants (16, 18). As shown in Fig. 2, *B* and *C*, both anti-NRT2.1 antibodies revealed several bands at ~45, ~75, and ~100–120 kDa. An additional band at ~60 kDa was found with the anti-NRT2.1 19 antibody, but not with the anti-NRT2.1 20 antibody. These bands were all specific for NRT2.1 because they were absent in the microsomes from the two *nrt2.1* knock-out mutants. For all the bands, the anti-NRT2.1 20 antibody always gave the strongest signal and was thus preferentially used in most of the experiments. In PM-enriched fractions, only the bands at ~45 and ~100–120 kDa were visible (Fig. 2*D*). With both antibodies the strong band observed at ~45 kDa was by far the most abundant form of NRT2.1 in both microsomes and PM because it could be readily observed after a few minutes of exposure to film. By contrast, several hours were required to get a visible signal for the other ones. It is likely that the band at ~45 kDa corresponds to the monomeric isolated form of NRT2.1. The apparent size of ~45 kDa differs from its theoretical molecular mass of 57 kDa. However, this may be due to the hydrophobic nature of the protein, as already seen with previously characterized sugar (48), ammonium (49), and nitrate transporters (50, 51), which

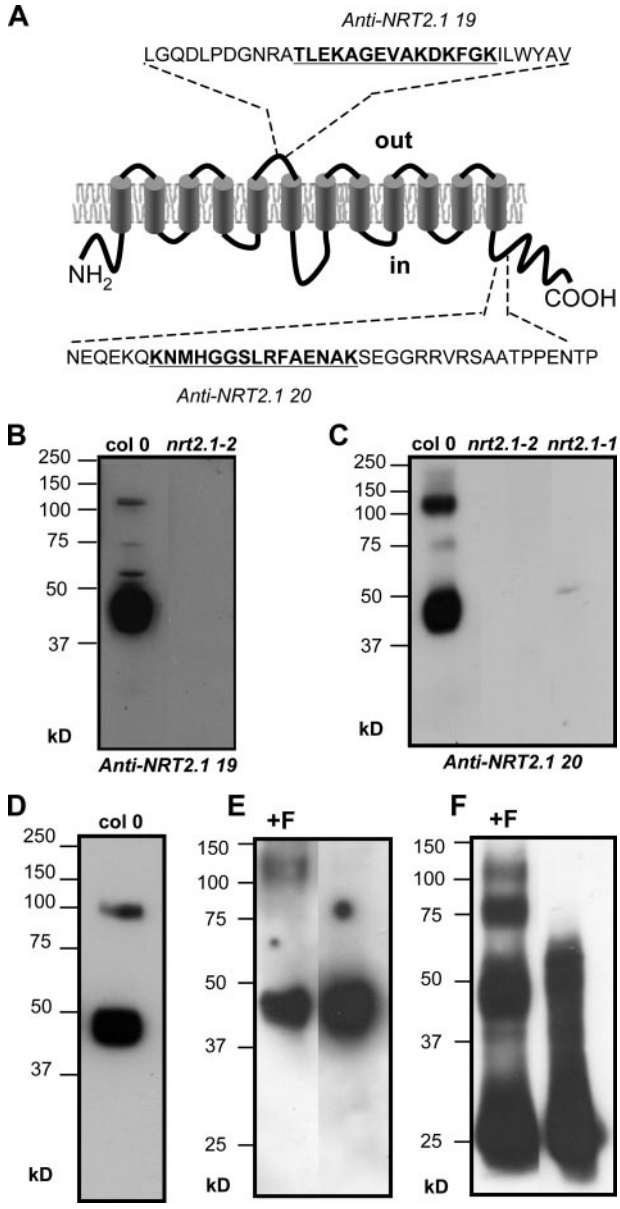

FIGURE 2. **Immunological analysis of NRT2.1 in root cell membranes.** *A*, membrane topology of NRT2.1 predicted by hydropathy analysis (3) with the peptidic sequences used to generate NRT2.1 antibodies called anti-NRT2.1 19 and anti-NRT2.1 20 (indicated in *bold*). *B* and *C*, immunoblot for NRT2.1 using total microsomes extracted from roots of 6-week-old hydroponically grown wild-type plants (*col 0*) and knock-out mutants for *NRT2.1* (*nrt2.1-1* and *nrt2.1-2*). Samples were separated on a 11% SDS-PAGE gel (5 μg of protein/lane). *D* and *E*, immunoblot for NRT2.1, and *F*, PIP2 (PIP2.1, PIP2.2, and PIP2.3) using plasma membranes extracted from roots of 6-week-old hydroponically grown plants. For *E* and *F*, half of the plants were treated with 1% formaldehyde (+*F*) for 45 min to induce *in vivo* protein cross-linking before plasma membrane extraction. Samples were separated on a 11% SDS-PAGE gel (4 μg of protein/lane).

all display in Western blots an apparent lower molecular mass than the theoretical one. The bands at ~75 and ~100–120 kDa may reveal higher molecular mass complexes incorporating NRT2.1. For simplicity, the highest molecular mass band is referred to as the ~120-kDa complex in the following text, although its apparent size was found to vary between 100 and 150 kDa, depending on the blots.

To make sure that the ~45-kDa band, corresponding to the isolated form of NRT2.1, is actually present in the native PM, and is not a product resulting from the dissociation of the higher molecular mass complexes, we performed *in vivo* cross-linking to stabilize protein complexes before PM extraction. Cross-linking was induced by adding 1% formaldehyde to the nutrient solution 45 min prior to harvesting for PM extraction. This markedly improved the detection of the band at ~120 kDa (Fig. 2*E*). However, this did not lead to the disappearance or a decrease in the intensity of the band at ~45 kDa, which remained strongly predominant in PM from plants treated with formaldehyde. As a control for the efficiency of protein-protein cross-linking, the same blot was probed with an anti-PIP2 antibody (Fig. 2*F*). PIP2 is a plasma membrane aquaporin that assembles in membranes as tetramers (52). Without cross-linking, only a monomer at 26–29 kDa and a dimer at 52 kDa of PIP2 were immunodetected on SDS-PAGE gels (43). By contrast a trimer at 75 kDa and a tetramer at 100 kDa were clearly immunodetected upon *in vivo* cross-linking. This last result validates the efficiency of formaldehyde-induced cross-linking.

Role of NAR2.1 in the Expression and Localization of NRT2.1—It has been recently suggested that the NO_3^- HATS in *Arabidopsis* may actually be a dual component transport system, involving both NRT2.1 and NAR2.1 proteins (19, 24, 25). Thus, a possibility would be that the high molecular mass bands at ~75 and ~120 kDa correspond to NRT2.1/NAR2.1 complexes. To investigate this hypothesis, we used the *nar2.1-1* knock-out mutant for *NAR2.1* (19) (also named *nrt3.1-2* in Ref. 25) to perform Western blots on microsomes in comparison with the wild-type Wassilewskija. Before extraction of microsomes, plants were treated with 1% formaldehyde during 45 min to induce *in vivo* protein cross-linking. The data obtained showed that the band at ~120 kDa is only slightly affected in the mutant *nar2.1-1* compared with the WT, whereas the band at ~75 kDa, and surprisingly the major one at ~45 kDa, disappeared completely in the mutant microsomes (Fig. 3, *A* and *B*). The absence of the major form of NRT2.1 in the *nar2.1-1* mutant was also found using PM fractions (data not shown), and was not due to a defect in *NRT2.1* gene expression because in our conditions, the *NAR2.1* mutation did not affect *NRT2.1* mRNA accumulation in the roots (Fig. 3*C*). Furthermore, the analysis of transgenic lines expressing a $P^{35}S$-*GFP-NRT2.1* transgene either in a wild-type, or in a *nar2.1-1* background confirmed this result because despite ectopic expression of the transgene, *NAR2.1* mutation resulted in an almost complete loss of GFP fluorescence associated with the PM (Figs. 3, *D–L*).

Regulation of NRT2.1 Abundance by Light, Sugars, and Nitrogen—To determine whether the abundance of NRT2.1 is regulated like *NRT2.1* expression and NO_3^- HATS activity, ELISA and Western blots were performed with PM or microsomes extracted from WT plants during a light/dark cycle and after various sugar or nitrogen treatments.

To study the regulation of NRT2.1 in response to light and sugars, PM were isolated from plants harvested at the end of a normal light period (5 p.m.), or after 4 h into the night (9 p.m.) with or without 1% sucrose supply (Fig. 4, *A–C*). These treatments strongly affect both *NRT2.1* mRNA accumulation and NO_3^- HATS activity because both decreases more than 50% after 4 h of darkness, but remain high when sucrose is supplied after the light/dark transition (30, 32) (Fig. 4*C*). Surprisingly,

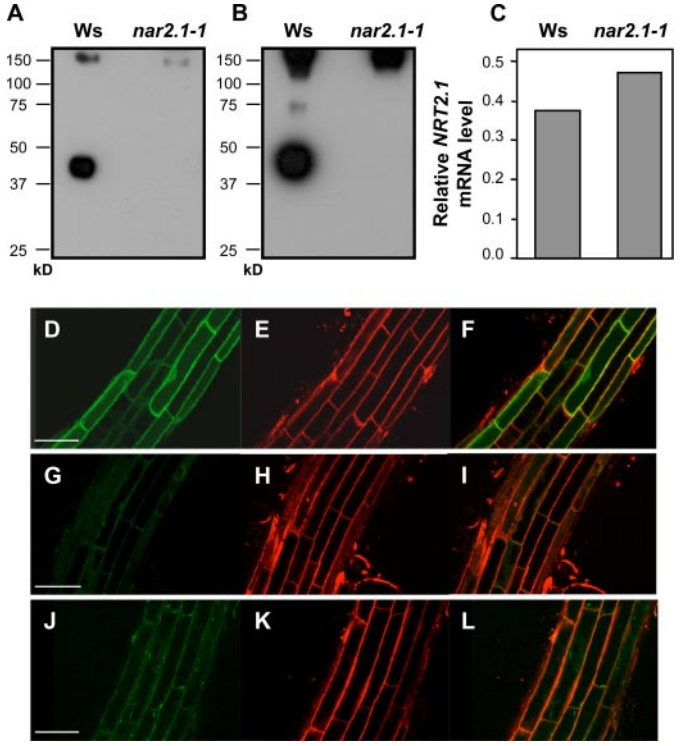

FIGURE 3. **NRT2.1 protein level and localization in the *nar2.1-1* mutant.** *A* and *B*, immunoblot for NRT2.1 using anti-NRT2.1 20 antibody and microsomes extracted from roots of 6-week-old hydroponically grown plants of WT (*Ws*, Wassilewskija) and *nar2.1-1* knock-out mutant. Plants were harvested at 1 p.m. after 4 h in the light. Before membrane extraction plants were treated with 1% formaldehyde for 45 min to induce *in vivo* protein cross-linking. Samples were separated on a 11% SDS-PAGE gel (6 μg of protein/lane). *A*, 4 min of exposure. *B*, one night of exposure. *C*, *NRT2.1* mRNA level measured by real-time quantitative PCR. Values are means of two independent replicates. Each value was normalized with the housekeeping gene Clathrin. *D–F*, GFP-NRT2.1 localization in plants expressing the *P*^{35}*S-GFP-NRT2.1* transgene in wild-type background (p43NRT2.1 plants), and *G–L*, in the *nar2.1-1* mutant background (two independent lines). Plants were grown in vertical Petri dishes for 7 days with 1% sucrose. *E*, *H*, and *K*, root cells were stained for 10 min with the endocytic tracer FM4-64. *F*, *I*, and *L*, overlay of the GFP and marker image. *Bar*, 40 μm.

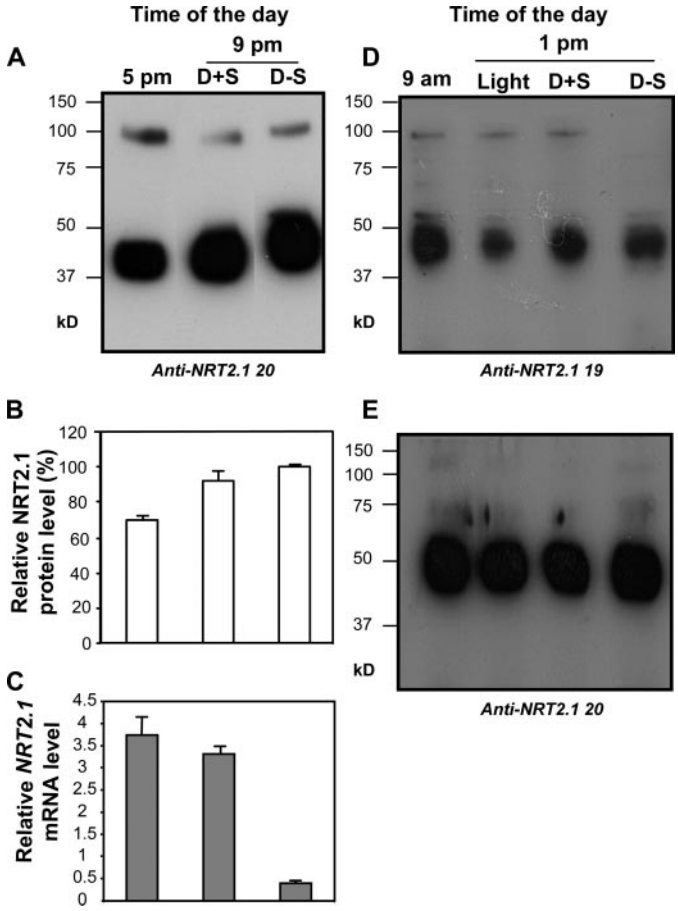

FIGURE 4. **Regulation of NRT2.1 level in response to light, dark, and sugar.** Roots of 6-week-old hydroponically grown plants were harvested during a normal day/night cycle at the end of the light period (5 p.m.) and after 4 h of darkness with (9 p.m. *D* + *S*) or without (9 p.m. *D* − *S*) 1% sucrose or at the end of the night period (9 a.m.) and after 4 h of light (1 p.m. light) or 4 h of prolonged darkness with (1 p.m. *D* + *S*) or without (1 p.m. *D* − *S*) 1% sucrose. *A*, immunoblot, and *B*, ELISA from two individual assays for NRT2.1 using plasma membranes. *C*, *NRT2.1* mRNA level measured by real-time quantitative PCR. Values are mean ± S.E. of two independent replicates. Each value was normalized with the housekeeping gene Clathrin. *D* and *E*, immunoblot for NRT2.1 using microsomes. Samples were separated on a 11% SDS-PAGE gel (4 μg of protein/lane).

Western blots did not reveal any significant changes in the abundance of the main form of NRT2.1 (at ~45 kDa) between the end of the light period and after 4 h in the dark with or without sucrose (Fig. 4*A*). Quantitative analysis by ELISA confirmed this result, showing that the total amount of NRT2.1 in the PM was not decreased after 4 h of darkness, and not increased by sugar supply in the dark (Fig. 4*B*). Furthermore, NRT2.1 abundance did not show any change at the beginning of the light period, when plants were illuminated for 4 h following the usual night period (Fig. 4, *D* and *E*). Sucrose supply also failed to increase the NRT2.1 level even during an extended 4-h dark period after the 16 h of normal night (Fig. 4, *D* and *E*). Concerning the band at ~120 kDa, it was detected in almost all PM extracts from plants in light or darkness, with roughly the same intensity (Fig. 4, *A* and *D*). These results, obtained with both anti-NRT2.1 antibodies, are representative of several independent experiments, leading to the conclusion that the abundance of NRT2.1 (at ~45 kDa) is neither regulated during the diurnal cycle, nor by short-term sucrose supply. Nevertheless, the amount of NRT2.1 in root PM did show a slight (but statistically significant) increase in response to light and sucrose supply following a 40-h prolonged period of darkness (supplemental materials Fig. S2). This increase remained, however, much lower than that observed at the mRNA level.

To further investigate the changes in NRT2.1 abundance in response to long-term treatments down-regulating both *NRT2.1* expression and NO_3^- HATS activity, we shifted to the study of the repressive effect of high nitrogen supply to the plants, because we found this more physiologically relevant than several days of extended darkness. Therefore, we compared hydroponically grown plants provided with 1 mM KNO_3 as a nitrogen source, or transferred either to nonrepressive, moderately repressive, or highly repressive media (0.3 mM KNO_3, 5 mM KNO_3, or 10 mM NH_4NO_3, respectively). These treatments are known to strongly affect *NRT2.1* mRNA accumulation within a few hours (11, 30, 33). A significant difference was observed in the abundance of both the main form of NRT2.1 at ~45 kDa and the protein complex at ~120 kDa in the root PM between plants supplied with 0.3 mM KNO_3 or 10 mM NH_4NO_3 for 7 days (Fig. 5, *C* and *D*). Both bands were clearly more intense under 0.3 mM KNO_3 conditions, suggest-

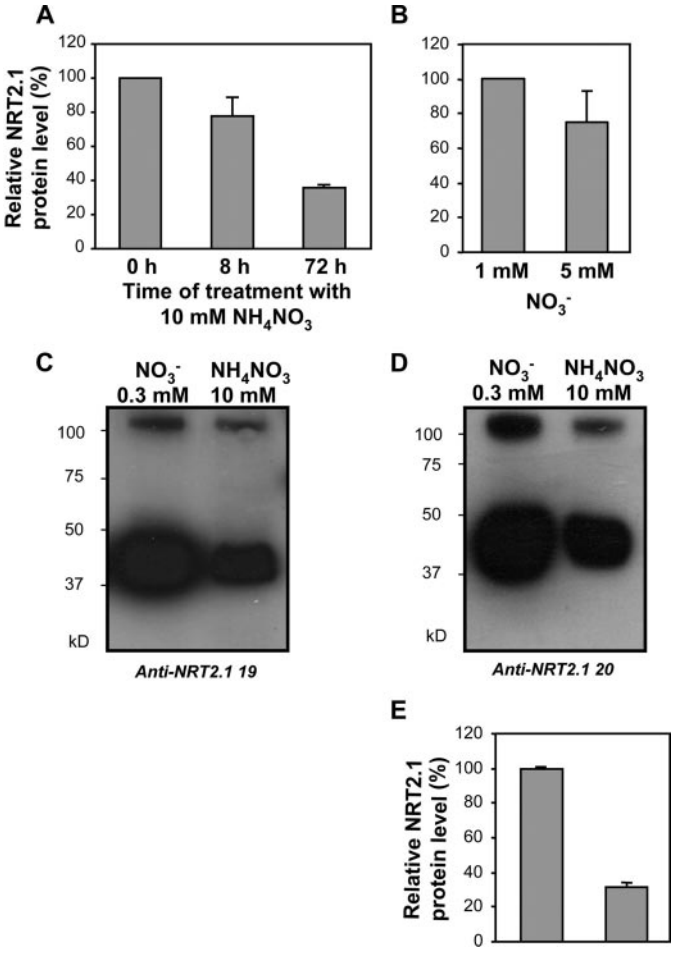

FIGURE 5. **Regulation of NRT2.1 level in response to low and high nitrogen nutrition.** *A* and *B*, ELISA from two individual assays for NRT2.1 using anti-NRT2.1 20 antibody and microsomes extracted from roots of 6-week-old hydroponically grown plants on 1 mM KNO_3 and transferred for 8 and 72 h (*A*) on 10 mM NH_4NO_3 or 72 h (*B*) on 5 mM KNO_3. *C* and *D*, immunoblot, and *E*, ELISA from two individual assays for NRT2.1 using PM from roots of 6-week-old hydroponically grown plants. PM were extracted from plants grown on 1 mM KNO_3 and transferred for 7 days on 0.3 mM KNO_3 or 10 mM NH_4NO_3. Samples were separated on a 11% SDS-PAGE gel (5 μg of protein/lane).

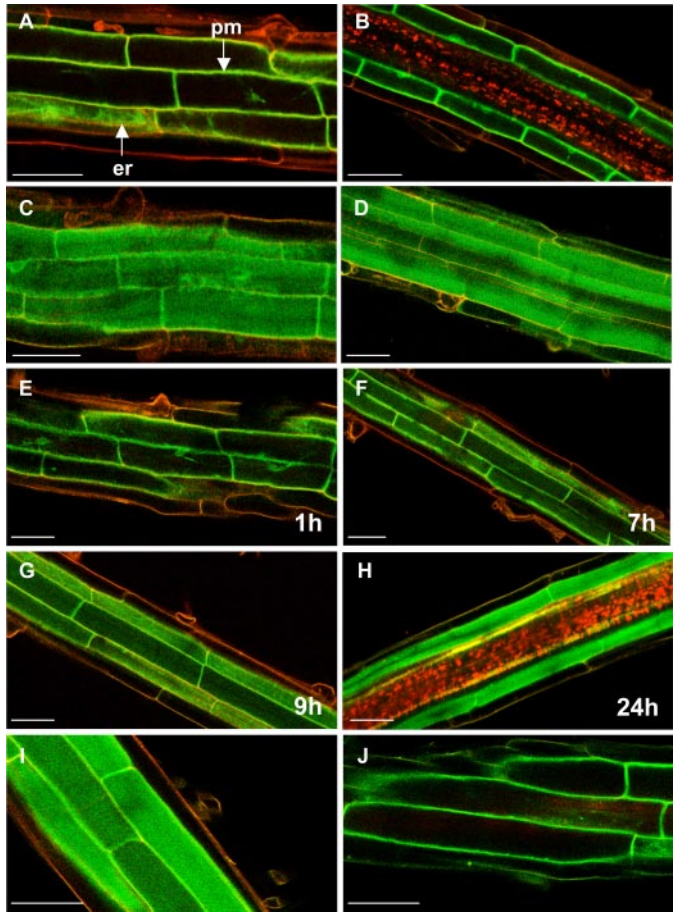

FIGURE 6. **Effect of light and sucrose on NRT2.1-GFP localization in the transgenic line GFP10.** Plants were grown in vertical Petri dishes for 14 days with or without 3% sucrose. GFP emission was detected on plants transferred for 24 h in the light with (*A*) or without (*B*) 3% sucrose or transferred during 24 h in the dark with (*C*) or without (*D*) 3% sucrose. The abbreviations used are: *pm*, plasma membrane; *er*, endoplasmatic reticulum. Time course studies were performed on plants grown without sucrose. They were transferred in the dark after 24 h of continuous light (*E–H*) or in the light after 24 h of continuous dark (*I* and *J*). GFP emission was measured 1 (*E*), 7 (*F*), 9 (*G*), and 24 (*H*) h after transfer of the plants in the dark and 0 (*I*) and 1.5 (*J*) h after transfer of the plants in the light.

ing regulation of the two forms of NRT2.1 by the nitrogen status of the plant. This result was confirmed by ELISA, indicating a 70% decrease in total NRT2.1 signal at 10 mM NH_4NO_3, compared with 0.3 mM KNO_3 (Fig. 5*E*). Time course experiments, however, indicated that a significant decay of NRT2.1 in response to high nitrogen required several days of treatment. Indeed, transfer of the plants from 1 mM NO_3^- to 10 mM NH_4NO_3 for 8 h or 3 days resulted in a 20 and 60% decrease in the total amount of NRT2.1, respectively (Fig. 5*A*). This repressive effect of high nitrogen supply was apparently not specifically due to the presence of NH_4^+ in the nutrient solution, because a moderate decrease of NRT2.1 abundance was also observed in response to the supply of 5 mM NO_3^- as the sole nitrogen source (Fig. 5*B*). Taken together, these data indicate that, unlike *NRT2.1* expression, NRT2.1 abundance is only slowly modified by light, sugar, or nitrogen treatments. This suggests that the NRT2.1 protein is relatively stable in the PM and remains abundant for hours or days after transcription of the gene has been down-regulated. This hypothesis is supported by the fact that the protein synthesis inhibitor cycloheximide has only a slow effect on NRT2.1 abundance in the PM, whereas it quickly reduced both *NRT2.1* mRNA level and $^{15}NO_3^-$ influx (supplemental materials Fig. S3).

Cleavage of the C Terminus of NRT2.1—To validate by another independent approach the conclusion that NRT2.1 abundance on PM is not regulated during the day/night cycle, we used GFP10 transgenic plants to determine how the NRT2.1-GFP protein responds to light and sugar. GFP10 plants were grown for 14 days on modified MS medium containing 1 mM KNO_3 with or without 3% sucrose. Plants were pre-treated for 24 h in the light or dark before confocal imaging. Under light conditions, GFP fluorescence was predominantly located in the PM and ER as described above, independently on the presence of sucrose (Fig. 6, *A* and *B*). Plants pre-treated for 24 h in the dark with or without sucrose also showed strong GFP fluorescence associated with PM/ER (Fig. 6, *C* and *D*). However, GFP fluorescence was also surprisingly strongly observed inside the cortical cells, filling a compartment, that most likely is the vac-

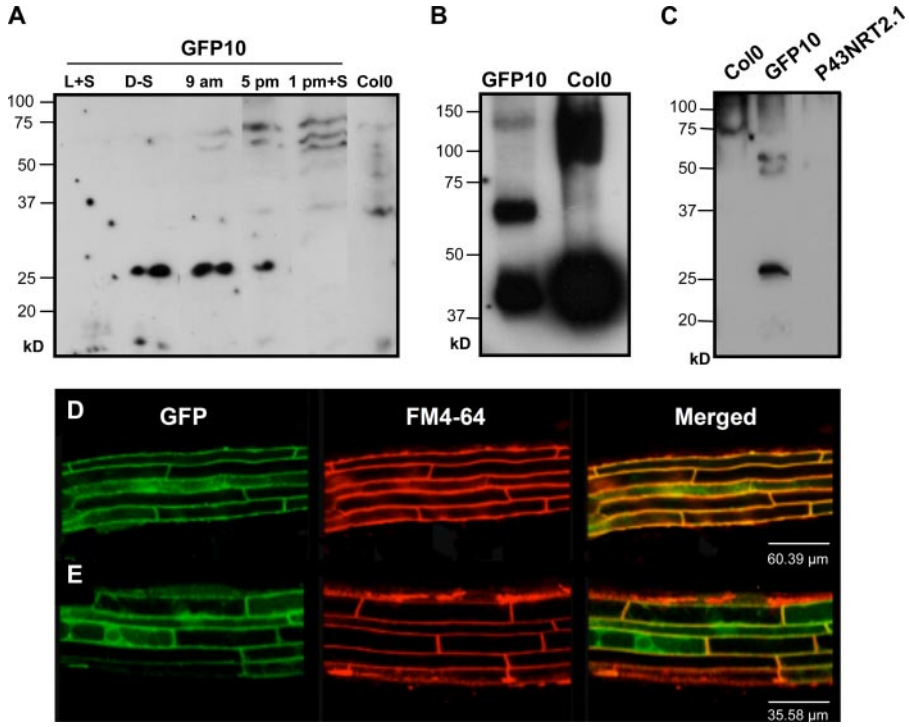

FIGURE 7. **Detection of NRT2.1 and GFP in roots of NRT2.1-GFP plants.** *A* and *C*, immunoblot for GFP in total protein extracts from roots of 6-week-old hydroponically grown plants of Col0, GFP10, and p43NRT2.1 (Wassilewskija wild-type transformed with the construct $P^{35}S$-GFP-NRT2.1). *A*, roots of GFP10 plants were harvested after a pre-treatment of 40 h in the dark and a treatment of 4 h in the light with 1% sucrose (*L* + *S*) or 4 h in the dark (*D* − *S*), during a day/night cycle at the end of the night (9 a.m.) or at the end of the light period (5 p.m.), and after a pre-treatment of 24 h in the light and a treatment of 4 h in the light with 1% sucrose (*1 pm* + *S*). Samples were separated on a 12% SDS-PAGE gel (50 µg of protein/lane). *B*, immunoblot for NRT2.1 in root plasma membranes of 6-week-old hydroponically grown plants of Col0 and GFP10. Roots were harvested after a pre-treatment of 24 h in the light and a treatment of 4 h in the light with 1% sucrose. Plants were treated for 45 min with 1% formaldehyde to induce *in vivo* protein cross-linking Samples were separated on a 10% SDS-PAGE gel (7 µg of protein/lane). *D* and *E*, GFP-NRT2.1 localization in plants expressing the *$P^{35}S$-GFP-NRT2.1* transgene in wild-type background (p43NRT2.1 plants). Plants were grown for 4 days in vertical Petri dishes on 1 mM KNO_3 and GFP emission was detected on plants transferred for an additional 24 h (*D*) in the light or 24 h in the dark (*E*).

uole (Fig. 6, *C* and *D*). Time course studies indicated that when plants were transferred in the dark after 24 h of continuous light, accumulation of GFP in the vacuole was observed after at least 9 h of darkness (Fig. 6, *E*–*G*), and increased until 24 h of darkness (Fig. 6*H*). In the reverse experiment, where plants were transferred to the light after 24 h of darkness, GFP fluorescence, which was observed both inside the vacuole and in the PM/ER of cortical cells at the beginning of the experiment (Fig. 6*I*), quickly disappeared from the inside of the cells after only 1 h 30 min of illumination (Fig. 6*J*), and stayed only visible in the PM/ER. The same results were found with GFP12 plants (results not shown).

To explain this observation Western blots were performed with soluble proteins and PM fractions extracted from WT and GFP10 plants using both anti-NRT2.1 and anti-GFP antibodies. As expected for a membrane protein, no signal was detected with anti-NRT2.1 antibody on the Western blot performed with soluble proteins (data not shown). However, using the same extract, a strong band was detected with the anti-GFP antibody, specifically in the GFP10 plants, at ~27–28 kDa (Fig. 7*A*), which fits exactly the molecular mass of free GFP. In agreement with the confocal microscopy data, the GFP band was only recorded at night, and quickly disappeared after only 4 h of light (Fig. 7*A*). This unexpected result suggests that the NRT2.1-GFP protein is cleaved, and that the GFP fluorescence seen inside the vacuole in the dark is due to free GFP generated by this cleavage. This conclusion is fully supported by Western blots performed with PM fractions of GFP10 plants using anti-NRT2.1 antibody. As shown in Fig. 7*B*, three specific bands were detected in the PM of GFP10 plants: a weak band at ~120 kDa corresponding to the high molecular mass complex observed in the WT, a strong band at ~65 kDa, specific for GFP10 plants, which approximately corresponds to the expected size of the NRT2.1-GFP fusion protein, and surprisingly a strong band at ~45 kDa, *i.e.* at the size of the native NRT2.1 protein in the WT. This last result was totally unexpected because no native NRT2.1 protein should be found in the PM from GFP10 plants as this line was obtained after transformation of the *nrt2.1-1* knock-out mutant (see Fig. 2, *B* and *C*). The simplest interpretation of these data is that the band found at ~45 kDa in GFP10 PM is the portion of the NRT2.1-GFP protein that remains after GFP has been cleaved off. Interestingly, free GFP was not found in transgenic plants expressing a GFP-NRT2.1 protein with GFP fused at the N terminus of NRT2.1 (Fig. 7*C*), and accordingly, no GFP fluorescence was recorded inside the root cortical vacuoles when these plants were transferred for 24 h in the dark (Fig. 7, *D* and *E*). Furthermore, no GFP is observed in the root vacuoles of transgenic plants expressing GFP alone under the control of the ^{35}S promoter (supplemental materials Fig. S4).

DISCUSSION

Tissular and Subcellular Localization of NRT2.1—Despite extensive studies describing NRT2.1 as a major component of the NO_3^- HATS in *A. thaliana* (4, 17, 18, 20, 30, 32), the cellular and subcellular localization of this protein remained unknown. To address this point we developed a GFP strategy using the *nrt2.1-1* knock-out mutant complemented with a transgene expressing NRT2.1 fused at the C terminus with a GFP tag. To avoid the loss of specific tissular localization, *NRT2.1-GFP* was expressed under the control of the native *NRT2.1* promoter (29). Two transgenic lines were used, GFP10 and GFP12, that were functionally complemented by the *NRT2.1-GFP* construct (supplemental materials Fig. S1). These results strengthen the fact that our imaging of NRT2.1-GFP accurately reflects the native cellular distribution of NRT2.1.

As expected for a NO_3^- transporter involved in uptake from the soil into the roots, GFP localization is found in the epidermal and cortical cells of mature roots, where the bulk of nutrient uptake into the symplasm occurs. These results are fully consistent with the localization of *NRT2.1* gene expression using β-glucuronidase (*GUS*) or luciferase (*LUC*) reporter genes (26, 29), and indicate no discrepancy between gene and protein expression territories.

At the subcellular level, NRT2.1 is predominantly localized in the PM. This was confirmed by both NRT2.1-GFP and GFP-NRT2.1 imaging (Figs. 1, 3, and 6) and immunological assays (Western blots and ELISA) performed with purified PM fractions (Figs. 2, 4, 5, and 7). Furthermore, membrane fractionation on sucrose gradients indicated that the monomeric form of NRT2.1 (at ~45 kDa) is specifically present on PM (38). This localization corresponds to what was found for the NRT2.1 homologue in the yeast *H. polymorpha* (37), and is in agreement with the hypothesis that NRT2.1 is involved in root NO_3^- influx from the external medium (15, 17, 18).

The Unexpected Structural Complexity of NRT2.1 in Root Cell Membranes—Western blots reveal that at least two forms of NRT2.1, detected with both NRT2.1 antibodies, seem actually present in the PM: a major form detected at ~45 kDa, and a much less abundant form with a higher mass at ~120 kDa (Fig. 2). It suggests that, in PM, NRT2.1 may be part of a protein complex of two or more associated proteins, but is mainly present in its isolated monomeric form at ~45 kDa. Furthermore, a third band at ~75 kDa was detected when Western blots were performed with microsomal fractions, suggesting that there is another complex involving NRT2.1, not predominantly localized on PM. This third form of NRT2.1 could correspond to the GFP fluorescence detected in the network of the ER in NRT2.1-GFP transgenic lines (Fig. 1). The most obvious candidate protein possibly involved in complex formation with NRT2.1 is NAR2.1. Indeed, recent studies have shown that in *Arabidopsis*, like in *C. reinhardtii* and barley, NRT2.1 needs to interact with the NAR2.1 protein to be functional (19, 23–25, 53). The physiological characterization of a *NAR2.1* knock-out mutant (*nar2.1-1*), provided *in planta* evidence that the absence of NAR2.1 reduces NO_3^--inducible high-affinity NO_3^- influx by more than 90%, even though *NRT2.1* is normally expressed (19, 25). Furthermore Orsel *et al.* (19) showed, using a mating based split-ubiquitin system, that the interaction between NRT2.1 and NAR2.1 occurs at the protein level. These data clearly suggest that NAR2.1 is involved in a protein-protein interaction with NRT2.1, and thus that the higher molecular mass bands found in our Western blots might be constituted of both proteins. Surprisingly, immunological studies of NRT2.1 expression in the *nar2.1-1* mutant revealed that disruption of *NAR2.1* does not dramatically affect the band at ~120 kDa, but leads to the complete disappearance of the band at ~45 kDa, corresponding to the major form of NRT2.1 (Fig. 3). Accordingly, GFP fluorescence recorded from GFP-NRT2.1 protein is considerably decreased in the *nar2.1-1* mutant background as compared with the wild-type background (Fig. 3). Thus, it is concluded from these data that NAR2.1 is not part of the high molecular mass complex at ~120 kDa, but is strictly required for expression of the main form of NRT2.1, at ~45 kDa.

As already mentioned by Orsel *et al.* (19), one hypothesis for the function of NAR2.1 is that this protein is involved in targeting NRT2.1 to the PM, thus playing a similar role as PHF1 and AXR4, which were recently shown to be responsible for the trafficking of PHT1 and AUX1 transporters from the ER to the PM (54, 55). The complete absence of the main form of NRT2.1 (~45 kDa) from the PM of *nar2.1-1* roots (Fig. 3) is consistent with this hypothesis, especially because it cannot be attributed to the lack of *NRT2.1* gene expression in the *nar2.1-1* mutant (Fig. 3*C*). However, there are two intriguing aspects of the *nar2.1-1* phenotype, which call for a more complex explanation. First, unlike PHT1 and AUX1, which are retained in the ER in the *phf1* and *axr4* mutants, respectively (54, 55), NRT2.1 is absent in the root microsomal fractions of the *nar2.1-1* mutant (Fig. 3), and GFP-NRT2.1 was not found to accumulate in the ER of root cells in the transgenic lines in *nar2.1-1* background (Fig. 3, *D–L*). This suggests that, if involved in NRT2.1 trafficking, NAR2.1 also plays a role in either stimulating NRT2.1 synthesis or preventing NRT2.1 degradation. In either case, this would correspond to a mechanism for controlling expression of membrane proteins that has not been described yet in plants. Second, the high molecular mass complex at ~120 kDa was still present in the *nar2.1-1* microsomal fraction (Fig. 3), indicating that this form of NRT2.1 does not depend on NAR2.1 to be expressed in root cell membranes.

Because their composition remains unknown, it is difficult to speculate about the physiological role of the high molecular mass complexes revealed by anti-NRT2.1 antibodies. However, these results raised an important question about the relationship between the presence of NRT2.1 in two different forms in root PM, and the fact that this protein has two distinct functions, in high-affinity root NO_3^- uptake on the one hand (17, 18), and in regulation of lateral roots initiation on the other hand (16, 26). The phenotype of the *nar2.1-1* mutant (19, 25) allows providing a partial answer to this. As the suppression of high-affinity NO_3^- influx in this mutant corresponds to the disappearance of the band at ~45 kDa and not to the band at ~120 kDa (Fig. 3), we hypothesize that the active form of NRT2.1 for NO_3^- transport across the PM most probably corresponds to the isolated monomeric form at ~45 kDa, which is also the most abundant form of NRT2.1. This also indicates that the presence of the high molecular mass form of NRT2.1 at ~120 kDa in root cell membranes is not sufficient *per se* to mediate high-affinity NO_3^- uptake by the roots.

Regulation of the NRT2.1 Protein—The strong correlation observed between the changes in root accumulation of *NRT2.1* transcript and those of root NO_3^- influx in response to light, sugar, and high nitrogen supply has suggested that the regulation of the NO_3^- HATS may mainly be accounted for by a transcriptional control of *NRT2.1* expression (11, 17, 29–31). However, so far, no studies at the protein level have been performed to confirm that NRT2.1 abundance in root PM follows similar changes as *NRT2.1* mRNA or NO_3^- HATS activity. Very surprisingly, our data provide ample evidence that this is not the case. Both immunological assays in wild-type plants and confocal microscopy analysis of NRT2.1-GFP in transgenic plants showed that neither the day/night cycle nor sugar treatments had a marked influence on the abundance of NRT2.1 in root

PM (Figs. 4 and 6, and supplemental materials Fig. S2), whereas these conditions strongly affect the *NRT2.1* mRNA level and NO_3^- influx (30, 32). Significant decrease in the amount of NRT2.1 is only observed in plants transferred for at least 3 days on high nitrogen (10 mM NH_4NO_3 or 5 mM NO_3^-) compared with plants grown on low nitrogen (0.3 or 1 mM NO_3^-) (Fig. 5). However, little change in the amount of NRT2.1 is observed after a short treatment (8 h) on high nitrogen, whereas this time scale is known to be largely sufficient to down-regulate both *NRT2.1* expression and NO_3^- HATS activity (11, 17). Even after 1 week on 10 mM NH_4NO_3, the 3-fold reduction of the NRT2.1 protein level is surprisingly limited compared with the decreases in *NRT2.1* mRNA level and root NO_3^- influx observed in the same conditions (20- and 10-fold, respectively).[4] This slow response of the protein to strongly repressive treatments can be explained by its relatively high stability, as suggested by the results from cycloheximide treatment. Interestingly, a relatively long half-life of the transporters involved in NO_3^- HATS has already been suggested from physiological studies with the inhibitor of functional protein synthesis fluorophenylalanine (56).

The fact that the amount of NRT2.1 in the PM does not change in response to environmental conditions that affect the *NRT2.1* mRNA level and NO_3^- influx is, to our knowledge, pretty unique compared with what is known for the regulation of other ion or water transporter proteins. Several examples concerning the iron transporter IRT1 (57), the high-affinity NO_3^- transporter from *Tuber borchii* (58), the sulfate transporter HVST1 from barley (59), the phosphate transporter PT1 from Medicago and tomato (60, 61), and aquaporines (62) all showed a correlation between the level of mRNA and the level of the protein in response to iron starvation, nitrogen availability, sulfate re-supply, phosphate starvation, and salinity, respectively. However, recent large-scale experiments showed that transcript levels undergo marked and rapid changes during diurnal cycles and after transfer to darkness, whereas changes in enzyme activities are smaller and delayed (63). This strongly suggests that in many cases additional regulation at the level of protein is required. Evidence for the occurrence of post-translational control of NRT2 proteins have been provided by the observations that NO_3^- HATS activity is repressed by high nitrogen supply in transgenic lines of *N. plumbaginifolia*, constitutively overexpressing *NRT2.1* and by an increase in internal NH_4^+ concentration in roots of barley treated with MSO, whereas transcript levels remains high (35, 36). A possible post-translational regulatory mechanism that can be considered for controlling NRT2.1 activity relates to the NRT2.1/NAR2.1 interaction. The requirement for co-expression of both proteins to yield NO_3^- HATS activity in *Xenopus* oocytes has highlighted the hypothesis of a two-component transporter (19, 24). Accordingly, association/dissociation of the NRT2.1/NAR2.1 complex may be an efficient way to modulate transport activity. Without excluding this hypothesis, we found no evidence for the presence of a NRT2.1/NAR2.1 complex in PM (Fig. 3). Alternatively, the presence of a number of conserved protein kinase C recognition motifs in the N- and C-terminal domains of NRT2.1 (3) may suggest that phosphorylation events are involved in regulating NRT2.1 activity in response to environmental cues, as it was shown to be the case for NRT1.1 (51).

Evidence for Partial Proteolysis of NRT2.1 at the C Terminus of the Protein—The GFP filling of the vacuole observed in the GFP10 transgenic lines after transfer of the plants to the dark (Fig. 6) initially suggested a mechanism for NRT2.1 degradation similar to that recently described for the YNT1 NO_3^- transporter of *H. polymorpha* (37). In this particular yeast species, YNT1 is ubiquitinylated in response to glutamine supply, and is transferred to the vacuole where it is rapidly degraded by a specific proteinase A. In our case we showed that the fluorescence that slowly appears in the vacuole in darkness is due to the free GFP generated by the cleavage of the NRT2.1-GFP protein (Fig. 7*A*) and not to NRT2.1 trafficking for degradation in the vacuole. This mechanism does not remove the NRT2.1 part of the tagged protein from the PM (Fig. 7*B*), suggesting that this partial proteolysis of NRT2.1-GFP occurred in the PM, and not after a transfer to the vacuole. Furthermore, GFP filling of the vacuole in the dark does not correspond to a decrease in the fluorescence observed in PM (Fig. 6). This makes a profound difference with what happens in *H. polymorpha*, where degradation of YNT1 in the vacuole was actually associated with the removal of this transporter from the PM (37). The fact that both the fluorescence in the vacuole and the free GFP in soluble proteins are not found after long dark treatment when GFP is fused in N terminus of NRT2.1 (Fig. 7), demonstrates that the free GFP generation is specific of the C terminus NRT2.1-GFP fusion protein. Furthermore, the NRT2.1 part of NRT2.1-GFP that remains in the PM is still recognized by the anti-NRT2.1 antibody (Fig. 7*B*), which targets an epitope located only 18 amino acids upstream of the C terminus of NRT2.1. Taken together, both data from GFP imaging and immunological studies with anti-NRT2.1 and anti-GFP antibodies are all consistent with the hypothesis that NRT2.1 is subject to partial proteolysis at its C terminus. With the native NRT2.1 protein, this partial degradation mechanism is thus expected to generate on the one hand, the same truncated NRT2.1 protein as with NRT2.1-GFP, and on the other hand, a short peptide corresponding to the C terminus of NRT2.1. Both native and truncated NRT2.1 proteins would be indistinguishable in our Western blots, due to their very similar size.

An important question is to determine whether the partial proteolysis of NRT2.1 constitutes a post-translational mechanism for regulating its activity. The fact that cleavage of NRT2.1-GFP is only apparent at night, when the NO_3^- HATS activity is down-regulated, may suggest that it is associated with NRT2.1 inactivation. However, several observations do not fit with this hypothesis. First, GFP localization in the vacuole resulting from cleavage of NRT2.1-GFP is not suppressed by sucrose supply (Fig. 6), whereas this treatment is very effective in preventing down-regulation of the NO_3^- HATS (30, 32). Second, it is not certain that partial proteolysis of NRT2.1 only occurs at night. Indeed, Tamura *et al.* (64) showed that GFP located in the vacuole can only be visualized in the dark because light, and especially blue light, induces a conformational change in the protein, followed by a rapid degradation by vacuolar

[4] T. Girin and M. Lepetit, unpublished results.

papain-type cysteine proteinases under acidic pH. Thus, it cannot be ruled out that in our case, NRT2.1-GFP is always cleaved, independently of light or darkness, but that cleaved GFP can only be observed in the vacuole in the dark because of its rapid degradation in the light. This rapid degradation of GFP under light conditions was confirmed by transferring GFP10 plants to the light after 24 h of darkness. Only 1.5 h after transfer to the light, no more fluorescence could be observed in the vacuole (Fig. 7). Independently of the putative role of the NRT2.1 C terminus cleavage, it is noteworthy that the GFP part of the NRT2.1-GFP protein generated by this cleavage moves to the vacuole, and does not remain confined to the cytoplasm and nucleus, as usually observed with free GFP (65), even in the dark (see supplemental materials Fig. S4). If still fused to GFP, the C-terminal peptide of NRT2.1 may be responsible for addressing the tag protein to the vacuole, suggesting trafficking of the NRT2.1 C-terminal part to this compartment in wild-type plants.

In conclusion, our data provide new insights on several important aspects of NRT2.1 function and regulation. First, the complexity of NRT2.1 function (NO_3^- transport and root development) seems to be associated with a structural complexity of this protein, with at least two, and possibly three, different forms of NRT2.1 present in roots PM. The confirmation of the existence and the investigation of the respective roles of these different NRT2.1 forms will certainly be a major issue for the future. Second, the monomeric form of the NRT2.1 protein is absent in the *nar2.1-1* mutant suggesting that NAR2.1 is essential for expression of the NRT2.1 protein in the PM. Third, the lack of correlation between regulation of *NRT2.1* expression and NO_3^- HATS on the one hand, and regulation of the NRT2.1 protein level on the other hand, suggests that post-translational mechanisms are crucial for the fast modulation of NO_3^- uptake in response to environmental changes, as it is also the case for the control of the first step of NO_3^- reduction catalyzed by nitrate reductase (66, 67). One such mechanism could correspond to a partial proteolysis of NRT2.1. All these mechanisms seem to be original and possibly specific to plants as they differ compared with what was found for the NO_3^- transporter YNT1 in the yeast *H. polymorpha* (37).

Acknowledgments—We thank Tony Miller and Mathilde Orsel for providing nar2.1-1 mutant seeds.

REFERENCES

1. Orsel, M., Filleur, S., Fraisier, V., and Daniel-Vedele, F. (2002) *J. Exp. Bot.* **53,** 825–833
2. Okamoto, M., Vidmar, J. J., and Glass, A. D. (2003) *Plant Cell Physiol.* **44,** 304–317
3. Forde, B. G. (2000) *Biochim. Biophys. Acta* **1465,** 219–235
4. Filleur, S., and Daniel-Vedele, F. (1999) *Planta* **207,** 461–469
5. Galvan, A., and Fernandez, E. (2001) *Cell Mol. Life Sci.* **58,** 225–233
6. Gao-Rubinelli, F., and Marzluf, G. A. (2004) *Biochem. Genet.* **42,** 21–34
7. Perez, M. D., Gonzalez, C., Avila, J., Brito, N., and Siverio, J. M. (1997) *Biochem. J.* **321,** 397–403
8. Quesada, A., Krapp, A., Trueman, L. J., Daniel-Vedele, F., Fernandez, E., Forde, B. G., and Caboche, M. (1997) *Plant Mol. Biol.* **34,** 265–274
9. Unkles, S. E., Hawker, K. L., Grieve, C., Campbell, E. I., Montague, P., and Kinghorn, J. R. (1991) *Proc. Natl. Acad. Sci. U. S. A.* **88,** 204–208
10. Unkles, S. E., Zhou, D., Siddiqi, M. Y., Kinghorn, J. R., and Glass, A. D. (2001) *EMBO J.* **20,** 6246–6255
11. Zhuo, D., Okamoto, M., Vidmar, J. J., and Glass, A. D. (1999) *Plant J.* **17,** 563–568
12. Crawford, N. M., and Glass, A. D. M. (1998) *Trends Plant Sci.* **3,** 389–395
13. Daniel-Vedele, F., Filleur, S., and Caboche, M. (1998) *Curr. Opin. Plant Biol.* **1,** 235–239
14. Williams, L., and Miller, A. (2001) *Annu. Rev. Plant Physiol. Plant. Mol. Biol.* **52,** 659–688
15. Li, W., Wang, Y., Okamoto, M., Crawford, N. M., Siddiqi, M. Y., and Glass, A. D. (2007) *Plant Physiol.* **143,** 425–433
16. Little, D. Y., Rao, H., Oliva, S., Daniel-Vedele, F., Krapp, A., and Malamy, J. E. (2005) *Proc. Natl. Acad. Sci. U. S. A.* **102,** 13693–13698
17. Cerezo, M., Tillard, P., Filleur, S., Munos, S., Daniel-Vedele, F., and Gojon, A. (2001) *Plant Physiol.* **127,** 262–271
18. Filleur, S., Dorbe, M. F., Cerezo, M., Orsel, M., Granier, F., Gojon, A., and Daniel-Vedele, F. (2001) *FEBS Lett.* **489,** 220–224
19. Orsel, M., Chopin, F., Leleu, O., Smith, S. J., Krapp, A., Daniel-Vedele, F., and Miller, A. J. (2006) *Plant Physiol.* **142,** 1304–1317
20. Orsel, M., Eulenburg, K., Krapp, A., and Daniel-Vedele, F. (2004) *Planta* **219,** 714–721
21. Zhou, J. J., Trueman, L. J., Boorer, K. J., Theodoulou, F. L., Forde, B. G., and Miller, A. J. (2000) *J. Biol. Chem.* **275,** 39894–39899
22. Koltermann, M., Moroni, A., Gazzarini, S., Nowara, D., and Tischner, R. (2003) *Plant Mol. Biol.* **52,** 855–864
23. Zhou, J. J., Fernandez, E., Galvan, A., and Miller, A. J. (2000) *FEBS Lett.* **466,** 225–227
24. Tong, Y., Zhou, J. J., Li, Z., and Miller, A. J. (2005) *Plant J.* **41,** 442–450
25. Okamoto, M., Kumar, A., Li, W., Wang, Y., Siddiqi, M. Y., Crawford, N. M., and Glass, A. D. (2006) *Plant Physiol.* **140,** 1036–1046
26. Remans, T., Nacry, P., Pervent, M., Girin, T., Tillard, P., Lepetit, M., and Gojon, A. (2006) *Plant Physiol.* **140,** 909–921
27. Crawford, N. M. (1995) *Plant Cell* **7,** 859–868
28. Stitt, M. (1999) *Curr. Opin. Plant Biol.* **2,** 178–186
29. Nazoa, P., Vidmar, J. J., Tranbarger, T. J., Mouline, K., Damiani, I., Tillard, P., Zhuo, D., Glass, A. D., and Touraine, B. (2003) *Plant Mol. Biol.* **52,** 689–703
30. Lejay, L., Tillard, P., Lepetit, M., Olive, F., Filleur, S., Daniel-Vedele, F., and Gojon, A. (1999) *Plant J.* **18,** 509–519
31. Gansel, X., Munos, S., Tillard, P., and Gojon, A. (2001) *Plant J.* **26,** 143–155
32. Lejay, L., Gansel, X., Cerezo, M., Tillard, P., Muller, C., Krapp, A., von Wiren, N., Daniel-Vedele, F., and Gojon, A. (2003) *Plant Cell* **15,** 2218–2232
33. Munos, S., Cazettes, C., Fizames, C., Gaymard, F., Tillard, P., Lepetit, M., Lejay, L., and Gojon, A. (2004) *Plant Cell* **16,** 2433–2447
34. Krouk, G., Tillard, P., and Gojon, A. (2006) *Plant Physiol.* **142,** 1075–1086
35. Fraisier, V., Gojon, A., Tillard, P., and Daniel-Vedele, F. (2000) *Plant J.* **23,** 489–496
36. Vidmar, J. J., Zhuo, D., Siddiqi, M. Y., Schjoerring, J. K., Touraine, B., and Glass, A. D. (2000) *Plant Physiol.* **123,** 307–318
37. Navarro, F. J., Machin, F., Martin, Y., and Siverio, J. M. (2006) *J. Biol. Chem.* **281,** 13268–13274
38. Chopin, F., Wirth, J., Dorbe, M. F., Lejay, L., Krapp, A., Gojon, A., and Daniel-Vedele, F. (2007) *Plant Physiol. Biochem.*, in press
39. Clough, S. J., and Bent, A. F. (1998) *Plant J.* **16,** 735–743
40. Rohila, J. S., Chen, M., Cerny, R., and Fromm, M. E. (2004) *Plant J.* **38,** 172–181
41. Santoni, V., Bellini, C., and Caboche, M. (1994) *Planta* **192,** 557–566
42. Giannini, J. L., Gildensoph, L. H., Reynolds-Niesman, I., and Briskin, D. P. (1987) *Plant Physiol.* **85,** 1129–1136
43. Santoni, V., Vinh, J., Pflieger, D., Sommerer, N., and Maurel, C. (2003) *Biochem. J.* **373,** 289–296
44. Lobreaux, S., Massenet, O., and Briat, J. F. (1992) *Plant Mol. Biol.* **19,** 563–575
45. Delhon, P., Gojon, A., Tillard, P., and Passama, L. (1995) *J. Exp. Bot.* **46,** 1585–1594
46. Clarkson, D. T., Gojon, A., Saker, L. R., Wiersema, P. K., Purves, J. V., Tillard, P., Arnold, G. M., Paans, A. J. M., Vaalburg, W., and Stulen, I. (1996) *Plant Cell Environ.* **19,** 859–868
47. Bolte, S., Talbot, C., Boutte, Y., Catrice, O., Read, N. D., and Satiat-Jeun-

emaitre, B. (2004) *J. Microsc.* (*Oxf.*) **214,** 159–173
48. Schneidereit, A., Scholz-Starke, J., and Buttner, M. (2003) *Plant Physiol.* **133,** 182–190
49. Loque, D., Yuan, L., Kojima, S., Gojon, A., Wirth, J., Gazzarrini, S., Ishiyama, K., Takahashi, H., and von Wiren, N. (2006) *Plant J.* **48,** 522–534
50. Guo, F. Q., Wang, R., Chen, M., and Crawford, N. M. (2001) *Plant Cell* **13,** 1761–1777
51. Liu, K. H., and Tsay, Y. F. (2003) *EMBO J.* **22,** 1005–1013
52. Verkman, A. S., and Mitra, A. K. (2000) *Am. J. Physiol.* **278,** F13–F28
53. Quesada, A., Galvan, A., and Fernandez, E. (1994) *Plant J.* **5,** 407–419
54. Dharmasiri, S., Swarup, R., Mockaitis, K., Dharmasiri, N., Singh, S. K., Kowalchyk, M., Marchant, A., Mills, S., Sandberg, G., Bennett, M. J., and Estelle, M. (2006) *Science* **312,** 1218–1220
55. Gonzalez, E., Solano, R., Rubio, V., Leyva, A., and Paz-Ares, J. (2005) *Plant Cell* **17,** 3500–3512
56. Behl, R., Tischner, R., and Raschke, K. (1988) *Planta* **176,** 235–240
57. Connolly, E. L., Fett, J. P., and Guerinot, M. L. (2002) *Plant Cell* **14,** 1347–1357
58. Montanini, B., Viscomi, A. R., Bolchi, A., Martin, Y., Siverio, J. M., Balestrini, R., Bonfante, P., and Ottonello, S. (2006) *Biochem. J.* **394,** 125–134
59. Hawkesford, M. J., and Wray, J. L. (2000) *Adv. Bot. Res.* **33,** 159–223
60. Chiou, T. J., Liu, H., and Harrison, M. J. (2001) *Plant J.* **25,** 281–293
61. Muchhal, U. S., and Raghothama, K. G. (1999) *Proc. Natl. Acad. Sci. U. S. A.* **96,** 5868–5872
62. Boursiac, Y., Chen, S., Luu, D. T., Sorieul, M., van den Dries, N., and Maurel, C. (2005) *Plant Physiol.* **139,** 790–805
63. Gibon, Y., Usadel, B., Blaesing, O. E., Kamlage, B., Hoehne, M., Trethewey, R., and Stitt, M. (2006) *Genome Biol.* **7,** R76
64. Tamura, K., Shimada, T., Ono, E., Tanaka, Y., Nagatani, A., Higashi, S. I., Watanabe, M., Nishimura, M., and Hara-Nishimura, I. (2003) *Plant J.* **35,** 545–555
65. Haseloff, J., Siemering, K. R., Prasher, D. C., and Hodge, S. (1997) *Proc. Natl. Acad. Sci. U. S. A.* **94,** 2122–2127
66. Finnemann, J., and Schjoerring, J. K. (2000) *Plant J.* **24,** 171–181
67. Kaiser, W. M., and Huber, S. C. (2001) *J. Exp. Bot.* **52,** 1981–1989